Electronic Supplementary Material (ESI) for Dalton Transactions.
This journal is © The Royal Society of Chemistry 2020

Supporting Information

Bistable spin-crossover in a new series of $[Fe(BPP\text{-}R)_2]^{2+}$ (BPP = 2,6-bis(pyrazol-1-yl)pyridine; R = CN) complexes

Kuppusamy Senthil Kumar,[a,b]* Nicolas Del Giudice,[a] Benoît Heinrich,[a] Laurent Douce,[a] and Mario Ruben[a,b,c]*

[a]Institut de Physique et Chimie des Matériaux de Strasbourg (IPCMS), CNRS-Université de Strasbourg, 23, rue du Loess, BP 43, 67034 Strasbourg cedex 2, France.

[b]Institute of Nanotechnology (INT), Karlsruhe Institute of Technology (KIT), Hermann-von-Helmholtz-Platz 1, 76344, Eggenstein-Leopoldshafen, Germany.

[c]Institute of Quantum Materials and Technologies (IQMT), Karlsruhe Institute of Technology (KIT), Hermann-von-Helmholtz-Platz 1, 76344, Eggenstein-Leopoldshafen, Germany.

*e-mail: kavinsenthil82@gmail.com; mario.ruben@kit.edu

Contents

S1. Representation of angular components of **1c**

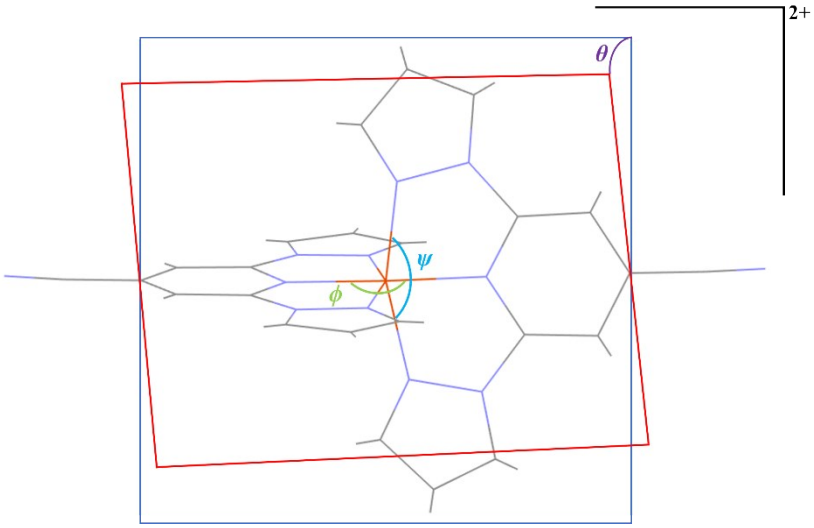

Chart S1. Structural model depicting angular components in $[Fe(1\text{-}BPP\text{-}CN)_2](BF_4)_2 \cdot CH_3CN$ (**1c**). The angles ϕ and θ represent the degree of distortion; complexes with ideal octahedral geometry have $\phi = 180°$ and $\theta = 90°$. The N{pyrazole}-Fe-N{pyrazole} clamp angle is represented as ψ.

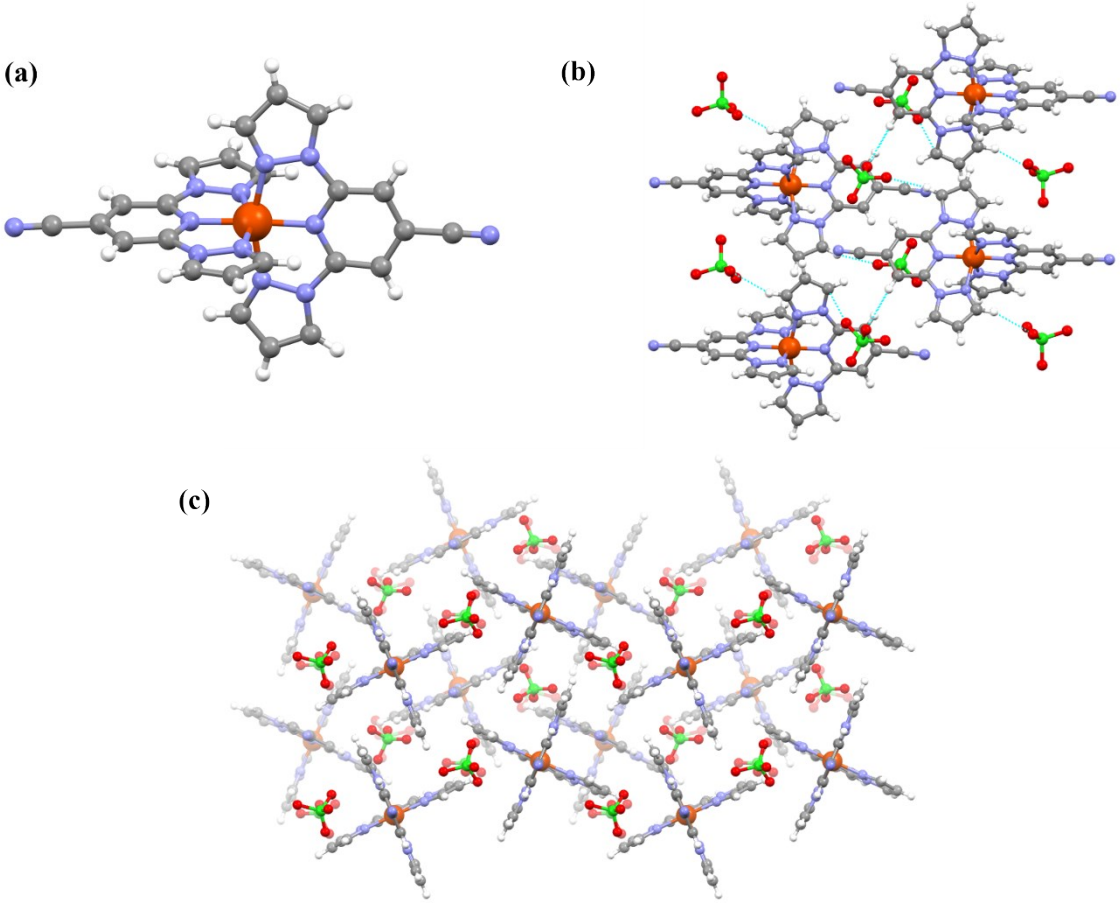

Figure S1. (a) X-ray structure of complex **2-cryst** (CCDC 2010806). Counter anions are omitted for clarity, (b) Intermolecular short contacts observed in the crystal lattice of **2-cryst**, and (c) Non-terpyridine embrace lattice packing pattern observed for complex **2-cryst** in the crystal lattice.

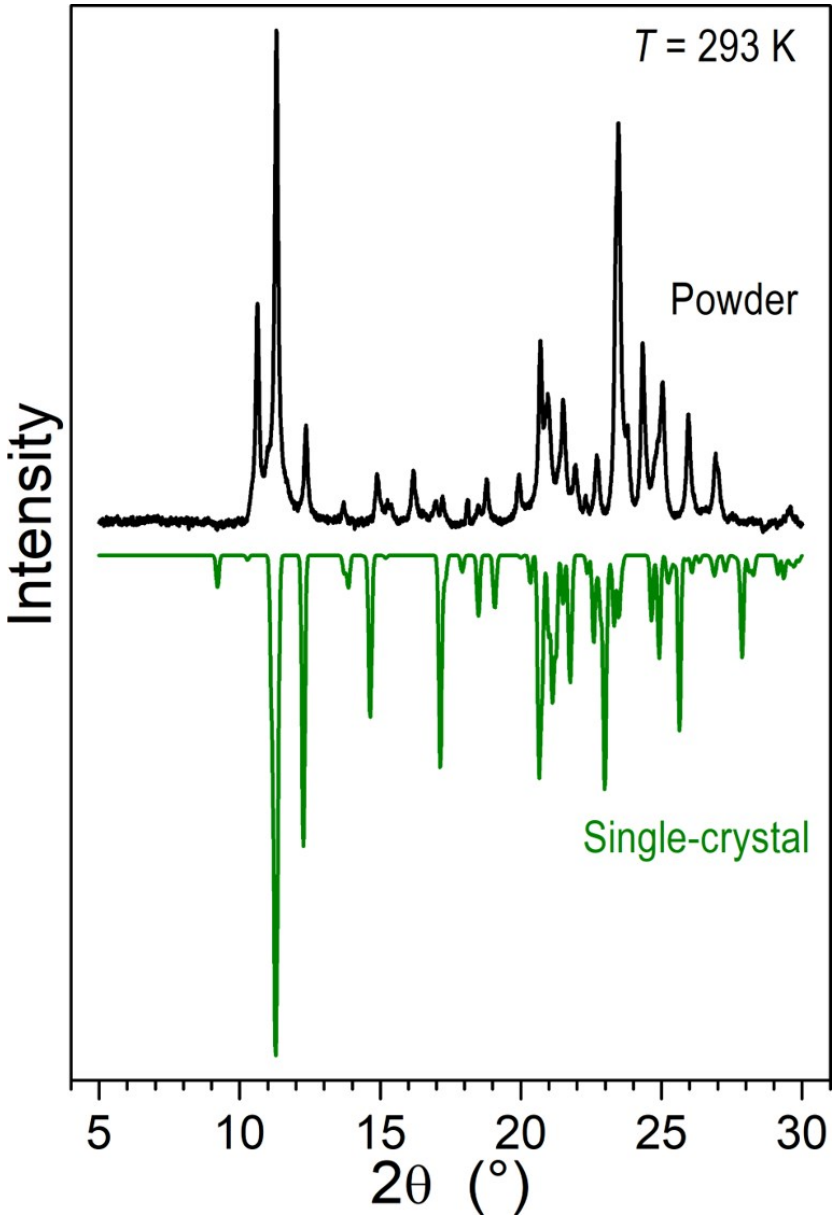

Figure S2. Comparison between the powder XRD pattern of **2** and SCXRD pattern of **2-cryst**. The remarkable difference between the patterns indicate different organizations of the molecules in the crystal lattice of **2** and **2-cryst**. Such different molecular organizations caused the HS and LS states of **2** and **2-cryst**, respectively, at 293 K.

S2. UV-vis spectra of the ligand and complexes **1a** and **2**

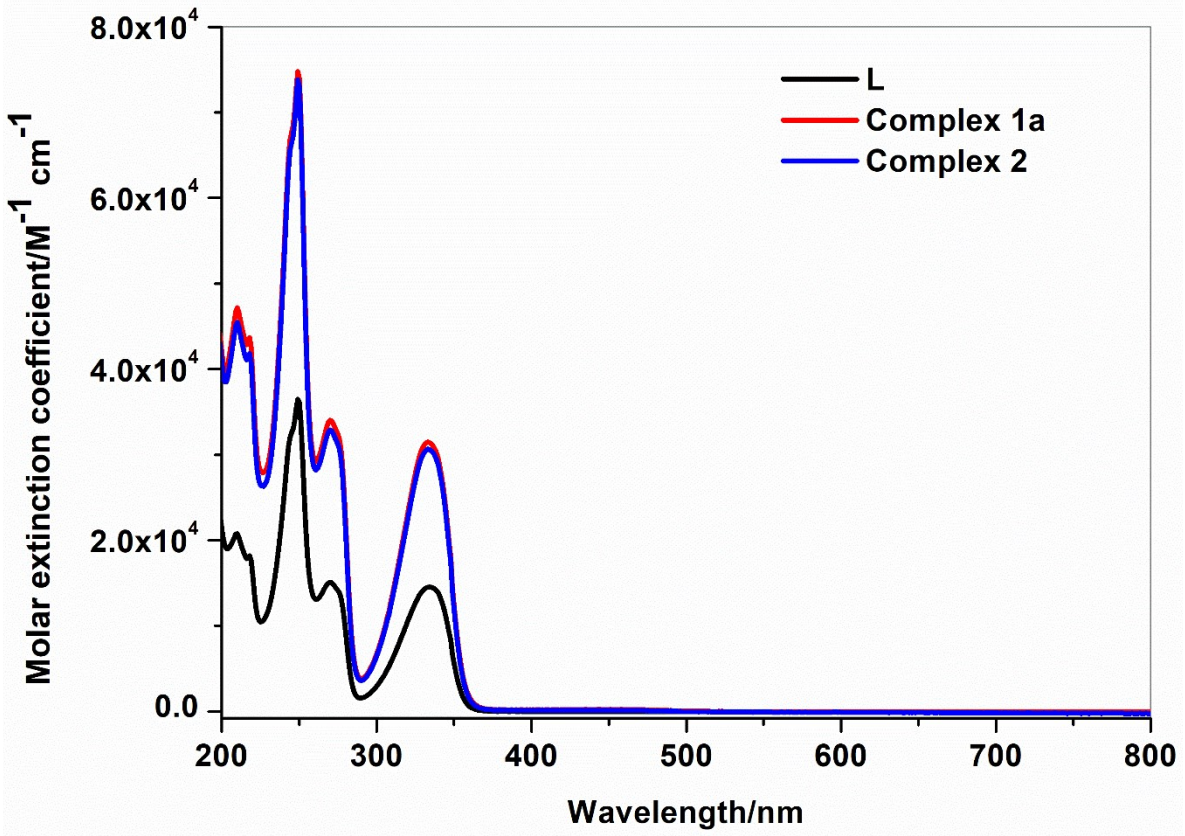

Figure S3. UV-vis absorption spectra of the ligand and complexes **1a** and **2**. Spectrophotometric grade acetonitrile was used as a solvent.

Table S1. Absorption maxima (λ_{max}) and molar extinction coefficients (ε) of the ligands and complexes

Entry	$\lambda_{max,abs}$ (ε) [nm, (10^4 M^{-1} cm^{-1})]
L	210 (2.06), 218 (1.82), 245 (3.21), 249 (3.66), 270 (1.48), 276 (1.36), 335 (1.47)
Complex **1a**	210 (4.7), 218 (4.34), 244 (6.72), 249 (7.49), 270 (3.41), 276 (3.2), 334 (3.18)
Complex **2**	210 (4.54), 218 (4.17), 245 (6.58), 249 (7.36), 270 (3.28), 276 (3.07), 333 (3.06)

S3. Spin-crossover characteristics of complexes **1b-d**

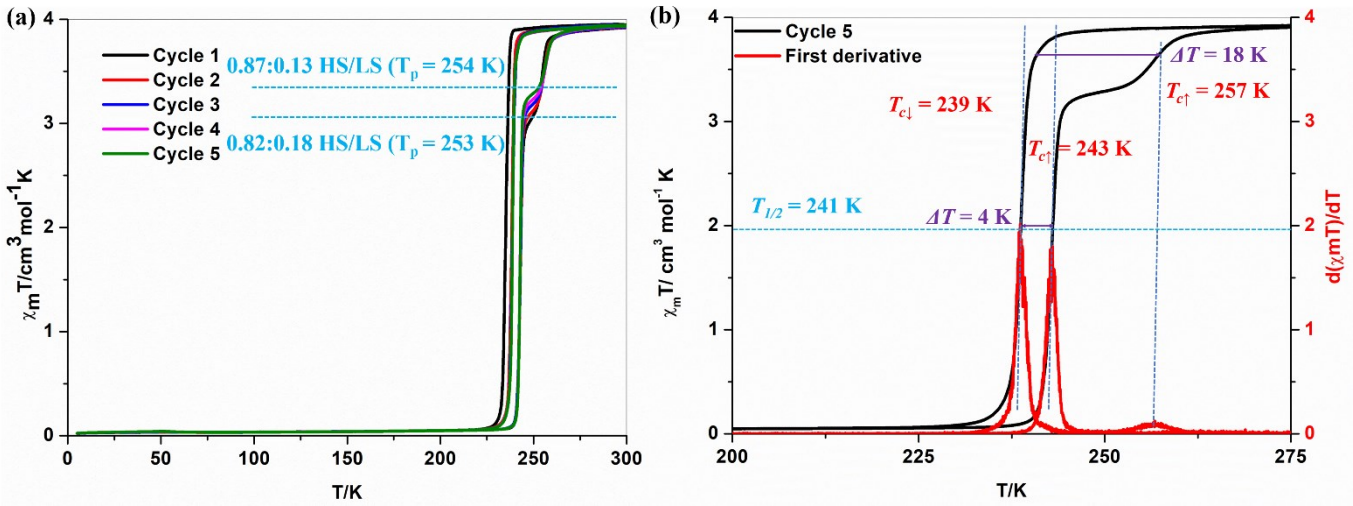

Figure S4. (a) $\chi_M T$ versus T plots of complex **1b**, and (b) $\chi_M T$ versus T and $d(\chi_M T)/dT$ versus T plots of complex **1b**, corresponding to cycle 5. T_p is the temperature, where the centre of the shoulder-like region situated. The critical temperatures (T_c) associated with the cooling and heating branches are designated as $T_{c\downarrow}$ and $T_{c\uparrow}$, respectively.

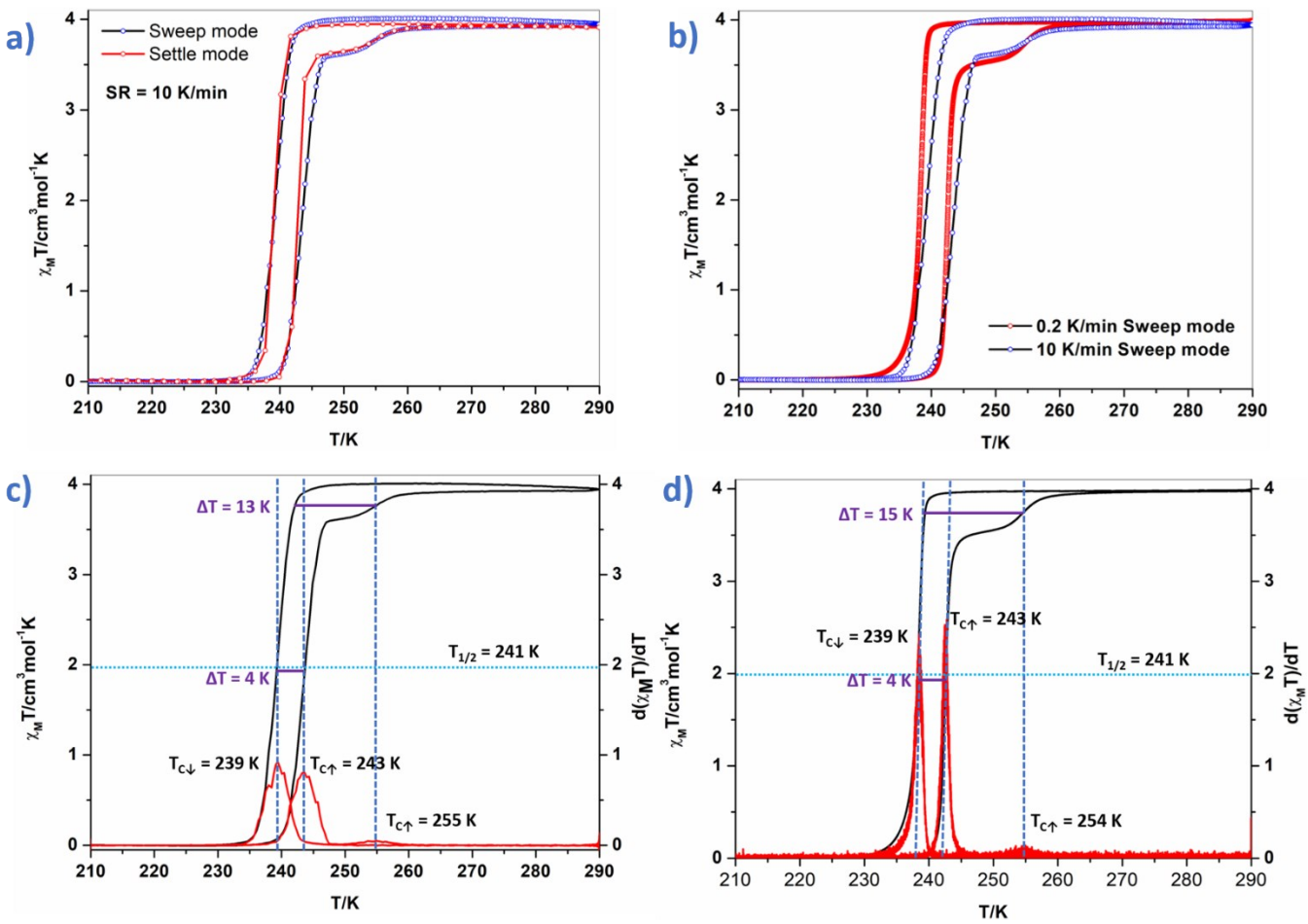

Figure S5. (a-b) $\chi_M T$ versus T plots of complex **1b** measured at scan rates of 0.2 K/min and 10 K/min. $\chi_M T$ versus T and $d(\chi_M T)/dT$ versus T plots of complex **1b** measured at (c) 10 K/min and (d) 0.2 K/min in sweep mode. The critical temperatures (T_c) associated with the cooling and heating branches are designated as $T_{c\downarrow}$ and $T_{c\uparrow}$, respectively. Note, the magnetic measurements with 0.2 K/min scan rate were performed in sweep mode. The comparable nature of $\chi_M T$ versus T profiles and ΔT = 4 K observed for both the scan rates in the sweep mode indicates scan rate independent nature of ΔT in **1b**.

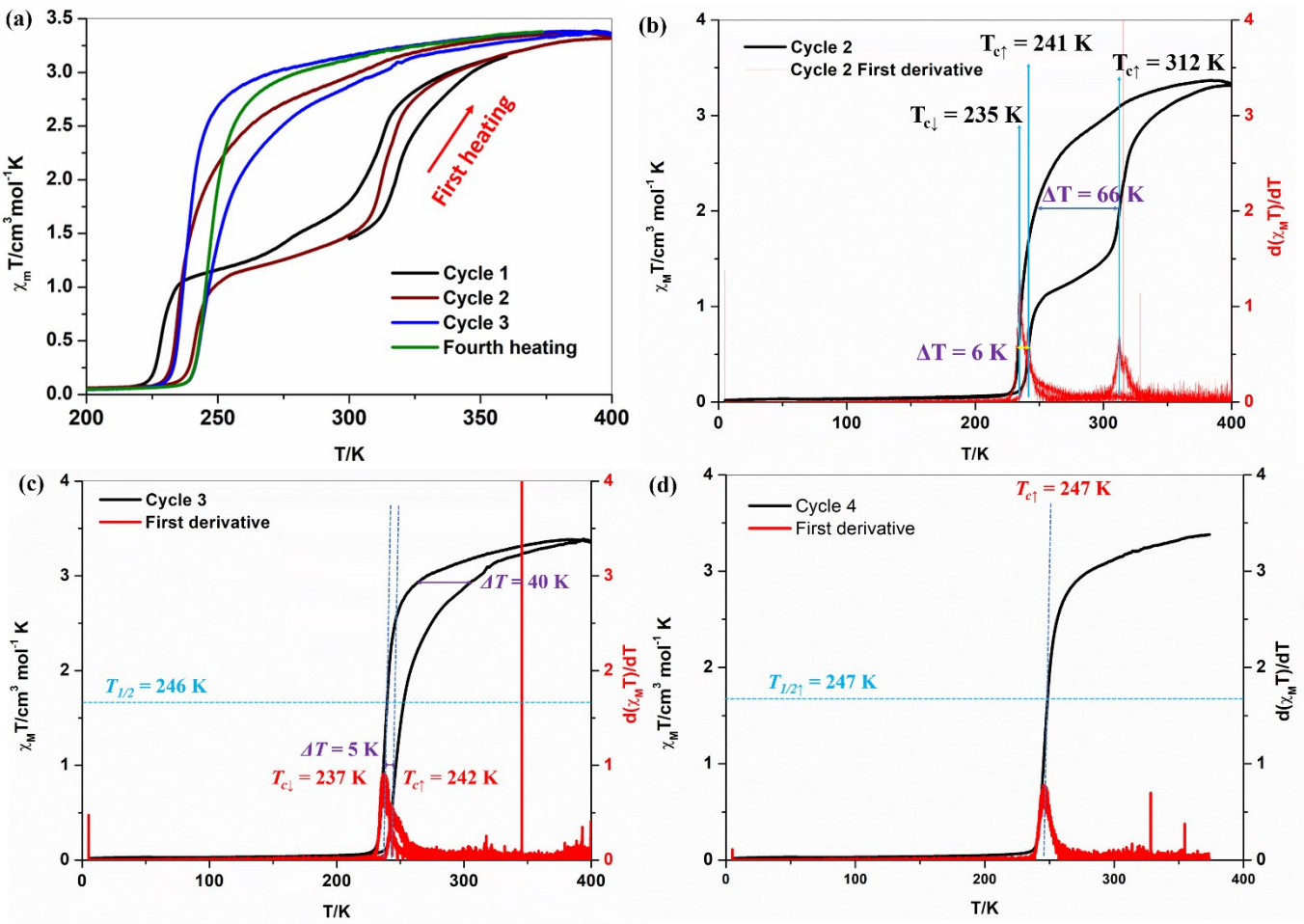

Figure S6. (a) $\chi_M T$ versus T plots and (b-c) $d(\chi_M T)/dT$ versus T and $\chi_M T$ versus T plots of complex **1c**. The critical temperatures (T_c) associated with the cooling and heating branches are designated as $T_{c\downarrow}$ and $T_{c\uparrow}$, respectively.

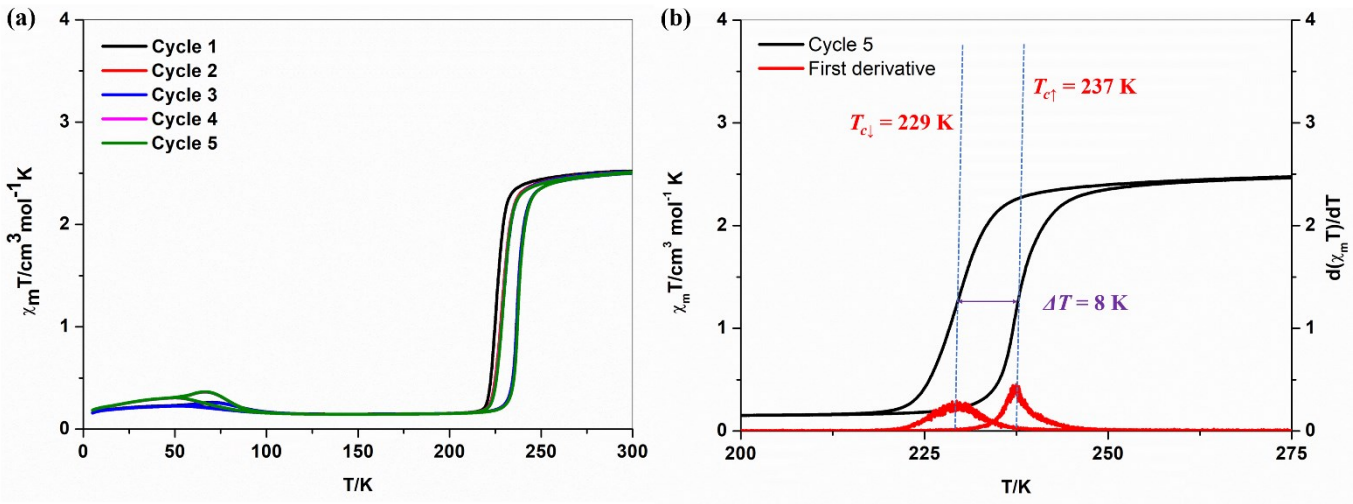

Figure S7. (a) $\chi_M T$ versus T plots, and (b) $d(\chi_M T)/dT$ versus T and $\chi_M T$ versus T plots of complex **1d** corresponding to cycle 5. The critical temperatures (T_c) associated with the cooling and heating branches are designated as $T_{c\downarrow}$ and $T_{c\uparrow}$, respectively.

S4. Differential scanning calorimetry studies of complexes 1c and 1d

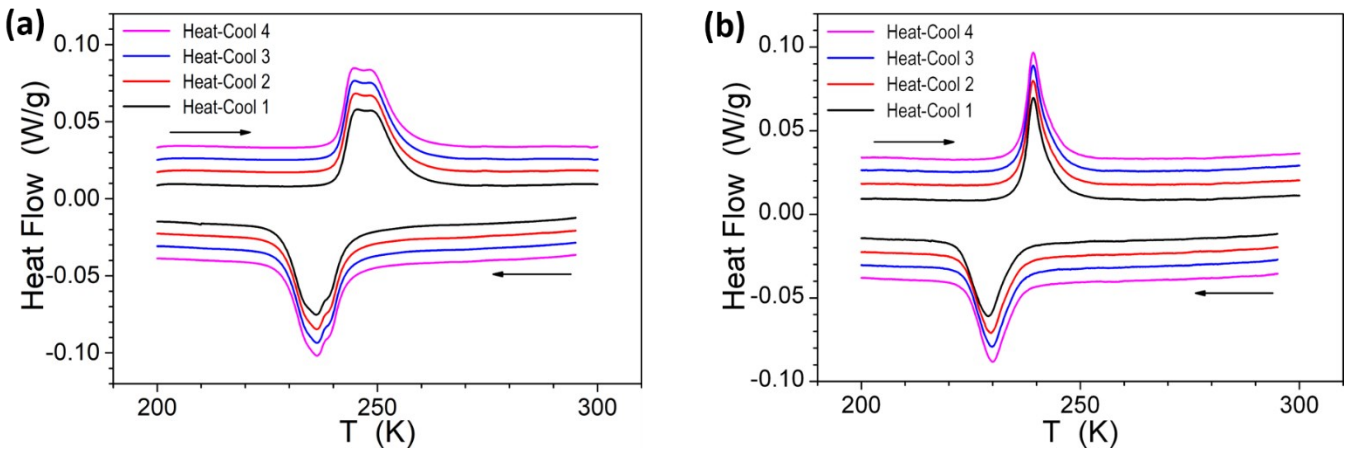

Figure S8. Differential scanning calorimetry (DSC) curves of complexes (a) solvent-free **1c** obtained after SQUID measurements and (b) **1d**. A scanning rate of 2 K/min, was employed; endotherm (up).